THE FASEB JOURNAL

RESEARCH ARTICLE

Compressive force-induced LincRNA-p21 inhibits mineralization of cementoblasts by impeding autophagy

Hao Liu[1] | Yiping Huang[1] | Yuhui Yang[1] | Yineng Han[1] | Lingfei Jia[2,3] | Weiran Li[1,4]

[1]Department of Orthodontics, Peking University School and Hospital of Stomatology, Beijing, China

[2]Central Laboratory, Peking University School and Hospital of Stomatology, Beijing, China

[3]Department of Oral and Maxillofacial Surgery, Central Laboratory, Peking University School and Hospital of Stomatology, Beijing, China

[4]National Engineering Laboratory for Digital and Material Technology of Stomatology, Beijing Key Laboratory of Digital Stomatology, Beijing, China

Correspondence
Lingfei Jia, Department of Oral and Maxillofacial Surgery, Central Laboratory, Peking University School and Hospital of Stomatology, 22 Zhongguancun Avenue South, Haidian District, Beijing 100081, P.R. China.
Email: jialingfei1984@sina.com

Weiran Li, Department of Orthodontics, Peking University School and Hospital of Stomatology, 22 Zhongguancun South Avenue, Haidian District, Beijing 100081, China.
Email: weiranli@bjmu.edu.cn

Abstract

The mineralization capability of cementoblasts is the foundation for repairing orthodontic treatment-induced root resorption. It is essential to investigate the regulatory mechanism of mineralization in cementoblasts under mechanical compression to improve orthodontic therapy. Autophagy has a protective role in maintaining cell homeostasis under environmental stress and was reported to be involved in the mineralization process. Long noncoding RNAs are important regulators of biological processes, but their functions in compressed cementoblasts during orthodontic tooth movement remain unclear. In this study, we showed that compressive force downregulated the expression of mineralization-related markers. LincRNA-p21 was strongly enhanced by compressive force. Overexpression of lincRNA-p21 downregulated the expression of mineralization-related markers, while knockdown of lincRNA-p21 reversed the compressive force-induced decrease in mineralization. Furthermore, we found that autophagy was impeded in compressed cementoblasts. Then, overexpression of lincRNA-p21 decreased autophagic activity, while knockdown of lincRNA-p21 reversed the autophagic process decreased by mechanical compression. However, the autophagy inhibitor 3-methyladenine abolished the lincRNA-p21 knockdown-promoted mineralization, and the autophagy activator rapamycin rescued the mineralization inhibited by lincRNA-p21 overexpression. Mechanistically, the direct binding between lincRNA-p21 and FoxO3 blocked the expression of autophagy-related genes. In a mouse orthodontic tooth movement model, knockdown of lincRNA-p21 rescued

the impeded autophagic process in cementoblasts, enhanced cementogenesis, and alleviated orthodontic force-induced root resorption. Overall, compressive force-induced lincRNA-p21 inhibits the mineralization capability of cementoblasts by impeding the autophagic process.

KEYWORDS

autophagy, biomechanical phenomena, cementogenesis, RNA, long noncoding, root resorption

1 | INTRODUCTION

External apical root resorption is one of the most frequent complications secondary to orthodontic treatment.[1] External apical root resorption has been reported to occur in all orthodontic patients,[2] while approximately 5% of patients experience over 5 mm of root shortening.[1] However, in the vast majority of patients, root shortening is slight and does not lead to severe clinical consequences due to the remineralization and cementogenesis of cementoblasts.[3] However, severe root resorption occurs when cementoblasts are incompetent.[4] Therefore, better insights into how orthodontic force regulates the mineralization capacity of cementoblasts are crucial for alleviating external apical root resorption during orthodontic tooth movement.

The mechanosensitivity of cementoblasts has been intensively reported.[5,6] It has been shown that mechanical force can impair the mineralization capability of cementoblasts by suppressing mineralization-related gene expression.[6] However, the underlying mechanism of how mechanical force regulates mineralization capability in cementoblasts remains unclear. Autophagy has been gradually regarded as an essential protective role in maintaining cell and tissue homeostasis under environmental stress, such as starvation and mechanical force.[7,8] Cells subjected to stress can survive with autophagic degradation of misfolded proteins, nonfunctional organelles, and intracellular pathogens.[9] Autophagy was reported to be increased in periodontal ligament stem cells under compressive force.[10] In contrast, Teng reported that moderate mechanical compression decreases the autophagic process in skeletal muscle cells and leads to increased apoptosis.[8] Accumulating evidence suggests that autophagy in osteoblasts is involved in mineralization and bone homeostasis.[11,12] However, no study has investigated the role of autophagy in the mineralization capability of compressive force-loaded cementoblasts.

Mammalian genomes encode thousands of long noncoding RNAs (lncRNAs), which are >200 nucleotides, distributed in the cytoplasm and nuclei.[13] LncRNAs regulate diverse cellular processes from normal development to disease progression.[13] Emerging studies have reported that

lncRNAs participate in the regulation of different cells responding to environmental stress.[5,14] Lu et al. reported that compressive force impeded the mineralization capability of osteoblasts by downregulating lncRNA Dancr expression.[14] Our previous study found that 57 lncRNAs showed upregulated expression and 13 showed downregulated expression in cementoblasts subjected to mechanical stress, indicating that lncRNAs may be involved in mechanical compression-induced variations in cementoblast functions.[5] LincRNA-p21, one of the lncRNAs with the strongest upregulation in expression, was identified as a transcriptional repressor of the p53-dependent apoptotic response[15] and was reported to regulate glycolytic metabolism.[16] However, whether and how lincRNA-p21 is involved in the regulation of cementogenesis needs further exploration.

Thus, in the present study, we performed in vivo and in vitro experiments to investigate whether and how mechanical stress-induced lincRNA-p21 is involved in the regulation of autophagy and cementogenesis during orthodontic tooth movement. Our results suggest potential therapeutic targets for preventing severe orthodontic root resorption.

2 | MATERIALS AND METHODS

2.1 | Animal experiments for orthodontic tooth movement

The experimental protocol was reviewed and approved by the Institutional Animal Care and Use Committee, Peking University (LA2021076). And this study conformed with the ARRIVE 2.0 guidelines. We made every effort to minimize the pain and stress that animals suffered in this trial. Healthy male C57BL/6 mice (6 weeks old, Vital River Laboratory Animal Technology Co., Beijing, China) weighing 20–25 g were used. Every 5 mice were maintained in a cage. The application of orthodontic force was modified on the basis of a previously described method.[17] In brief, after general anesthesia, nickel-titanium coil springs were applied to connect the maxillary right first molar and the incisors (Figure 1A), and then, a force of 20 g was exerted continuously. To
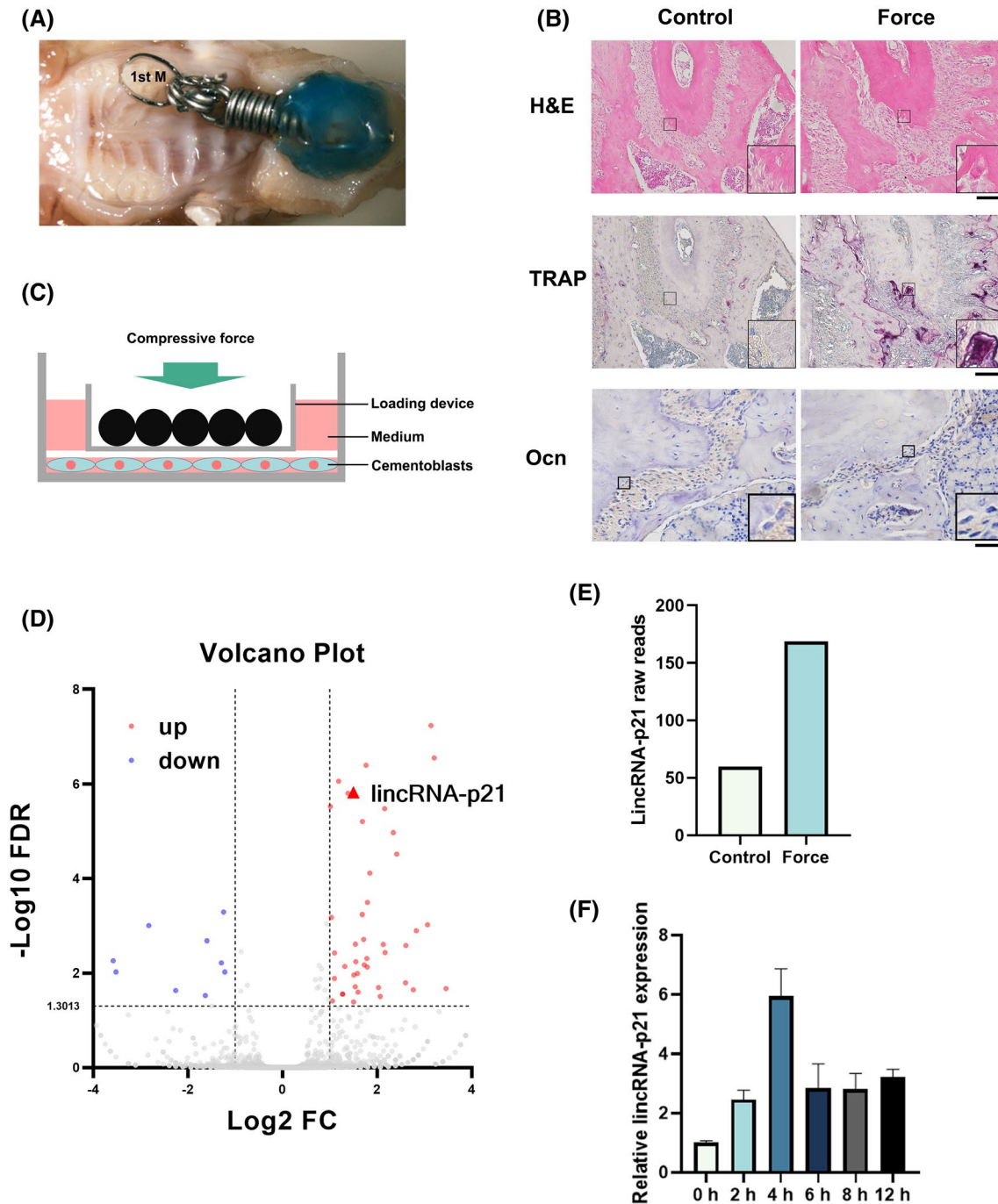
FIGURE 1 Orthodontic force led to root resorption in vivo, and compressive force upregulated lincRNA-p21 expression in vitro. (A) A picture of the mouse orthodontic tooth movement model. (B) Representative HE staining and TRAP staining images (scale bar: 100 μm). Representative immunohistochemical images of Ocn (scale bar: 50 μm). (C) Schematic diagram showing the application of compressive force. (D) Volcano plots of differentially expressed lncRNAs in compressed cementoblasts. (E) Relative expression of lincRNA-p21 measured by RNA sequencing in compressed cementoblasts. (F) Relative lincRNA-p21 expression in cementoblasts subjected to mechanical compression at 1.5 g/cm^2 for different durations (0, 2, 4, 6, 8 and 12 h; *$p < .05$)

ensure the consistency of force magnitudes, all force loading procedures were performed by the same experimenter. After 9 days, all mice were euthanized via overdose injection of sodium pentobarbital, and the maxillae were harvested and immersed in 4% paraformaldehyde for further experiments.

2.2 | Cell culture and pressure application

Immortalized mouse cementoblast-like cells were cultured in Dulbecco's modified Eagle's medium (Gibco, Grand Island, New York, USA) containing 10% fetal bovine serum (Gibco) and 1% penicillin/streptomycin

(Invitrogen, Carlsbad, California, USA) at 37°C with 5% CO_2. The compressive force was exerted as described previously.[5] In brief, after reaching 80% confluency, the cell layer was mechanically compressed using a glass cover with an additional plastic bottle containing steel balls on top (Figure 1C). An appropriate number of steel balls was applied to exert a compressive force of 1.5 g/cm^2.

2.3 | RNA sequencing and data analysis

The differentially expressed genes were identified as follows: (1) fold change >1.5 or fold change <0.6667 and (2) false discovery rate <0.05. Pathway analysis was used to assess the functions of co-expressed genes based on the Kyoto Encyclopedia of Genes and Genomes (KEGG) database. Raw RNA-Seq experimental data were uploaded to the Gene Expression Omnibus (GEO) public database (Accession No. GSE116785).

2.4 | Plasmids, RNA oligoribonucleotides and cell transfection

The lincRNA-p21 expression plasmid was constructed using the pQLL vector by Qinglan Biotech Co. (Wuxi, China) and named pQLL-lincRNA-p21. The pQLL vector was used as a negative control (pQLL-NC).

Small interfering RNAs (siRNAs) against lincRNA-p21 (si-lincRNA-p21), siRNAs against FoxO3 (siFoxO3), and scrambled control (siNC) were purchased from GenePharma Co. (Shanghai, China).

The sequences of lincRNA-p21 and siRNAs are listed in Table 1.

Lipofectamine 3000 (Invitrogen, Carlsbad, California, USA) was utilized to perform the transfection of plasmids and siRNAs, following the manufacturer's protocols. The RNA extractions were performed 24 h later, and protein extractions were performed 48 h later.

2.5 | Subcellular fractionation

Cytoplasmic and nuclear RNA were collected using a Nuclei Isolation kit (Invent Biotechnologies) according to the kit's manuals.

2.6 | RNA immunoprecipitation

RNA immunoprecipitation (RIP) was performed using a BersinBioTM RIP Kit (BersinBio, China) following the manufacturer's protocols. Briefly, cementoblasts were harvested, washed, and lysed in ice-cold lysis buffer. After

TABLE 1 SiRNA sequences used for RNA knockdown

SiRNA sequence	Sequence (5′−3′)
Si NC (sense)	UUCUCCGAACGUGUCACGUTT
Si NC (antisense)	ACGUGACACGUUCGGAGAATT
Si lincRNA-p21 1 (sense)	GCGAGAGCAUUGACACUUATT
Si lincRNA-p21 1 (antisense)	UAAGUGUCAAUGCUCUCGCUA
Si lincRNA-p21 2 (sense)	GGUUCUGUCUGCACCUCAUTT
Si lincRNA-p21 2 (antisense)	AUGAGGUGCAGACAGAACCCU
Si lincRNA-p21 3 (sense)	CCAGAACUGGAGCCAACAATT
Si lincRNA-p21 3 (antisense)	UUGUUGGCUCCAGUUCUGGUC
Si FoxO3 1 (sense)	GGCUCACUUUGUCCCAGAUTT
Si FoxO3 1 (antisense)	AUCUGGGACAAAGUGAGCCTT
Si FoxO3 2 (sense)	GCUCUUGGUGGAUCAUCAATT
Si FoxO3 2 (antisense)	UUGAUGAUCCACCAAGAGCTT
Si FoxO3 3 (sense)	GCCAGUCUAUGCAAACCCUTT
Si FoxO3 3 (antisense)	AGGGUUUGCAUAGACUGGCTT

centrifugation, the supernatant was incubated with FoxO3 antibody or control IgG for 16 h at 4°C. Then, the mixture was incubated with prepared protein A/G beads for 1 h at 4°C. After that, the beads were washed, and proteinase K was used to remove proteins. After extraction and purification, the RNA was subjected to quantitative real-time polymerase chain reaction (qRT-PCR) analysis. The antibodies used in RIP included FoxO3 (Cell Signaling Technology, Beverly, MA) and IgG (BersinBio, China).

2.7 | Quantitative real-time polymerase chain reaction

Cells were rinsed and harvested. TRIzol reagent (Invitrogen) was used to extract total RNA as described in the manufacturer's instructions. After that, the RNA was reverse-transcribed into complementary DNA (cDNA) using a PrimeScriptTM RT reagent Kit (TaKaRa, Tokyo, Japan). QRT-PCR was performed using SYBR Green Q-PCR Master Mix (Applied Biosystems, Foster City, California, USA) on an ABI Prism 7500 Real-Time PCR System (Applied Biosystems, Foster City, CA). The housekeeping gene glyceraldehyde-3-phosphate dehydrogenase (Gapdh) was used as the internal control. The relative RNA expression level was calculated using the delta-delta CT method. All primer pairs are listed in Table 2.

2.8 | Western blot

Cells were washed, harvested, and lysed in cold, freshly prepared radioimmunoprecipitation assay buffer (RIPA, Thermo Fisher Scientific, Waltham, MA) with a protease inhibitor

TABLE 2 Primer sequences used for real-time quantitative RT-PCR

qRT-PCR primer name	Primer sequence (5′–3′)
Gapdh (forward)	CAGGAGGCATTGCTGATGAT
Gapdh (reverse)	GAAGGCTGGGGCTCATTT
lincRNA-p21 (forward)	GACCAGAACTGGAGCCAACAA
lincRNA-p21 (reverse)	CCAGAGGTGAACTGCCTTCC
Bsp (forward)	AAAGTGAAGGAAAGCGACGA
Bsp (reverse)	GTTCCTTCTGCACCTGCTTC
Ocn (forward)	ACCCTGGCTGCGCTCTGTCTCT
Ocn (reverse)	GATGCGTTTGTAGGCGGTCTTCA
Osx (forward)	ATGGCGTCCTCTCTGCTTG
Osx (reverse)	TGAAAGGTCAGCGTATGGCTT
Runx2 (forward)	ATGCTTCATTCGCCTCACAAA
Runx2 (reverse)	GCACTCACTGACTCGGTTGG

cocktail (Solarbio, Beijing, China). A BCA Protein Assay kit (Solarbio, Beijing, China) was used to measure the protein concentration. The samples (30 µg) were separated by 8%–15% SDS-polyacrylamide gel electrophoresis and then transferred onto polyvinylidene fluoride membranes (PVDF, Millipore, USA) for immunoblotting. The membranes were blocked with 5% bovine serum albumin (BSA; Sigma–Aldrich, St. Louis, MO) and incubated with a primary antibody at 4°C overnight. The next day, the membranes were incubated with a secondary antibody for 1 h at room temperature. A chemiluminescence kit (Applygen, Beijing, China) was used to visualize the protein bands. Antibodies were as described in Table S1.

2.9 | Immunofluorescence staining

Cells were fixed with 4% paraformaldehyde at room temperature for 15 min. Then, 0.1% Triton X-100 was employed to permeabilize these cells for 15 min. After that, the cells were blocked with 5% BSA and incubated with a primary antibody at 4°C overnight. The next day, a specified secondary antibody was applied at room temperature for 1 h. The cell nuclei were counterstained with 4′,6-diamidino-2-phenylindole (DAPI, Zhongshan Goldenbridge Biotechnology Co.). A confocal imaging system (Carl Zeiss, Jena, Germany) was used to capture pictures. Antibodies were as described in Table S1.

2.10 | Lentivirus construction and functional analysis in vitro and in vivo

Negative control shRNA (5′-TTCTCCGAACGTGTCACG T-3′) and specific shRNA targeting lincRNA-p21 (5′-GCC

CTTAGGAATCCCTGAAAG-3′) were designed by Gene-Pharma Co. (Shanghai, People's Republic of China). Corresponding lentiviruses (Lv-shNC and Lv-shlincRNA-p21) were purchased from GenePharma. Cementoblasts were seeded in six-well plates and infected with Lv-shNC or Lv-shlincRNA-p21 following the manufacturer's instructions. qRT–PCR was performed to assess the efficiency of these lentiviruses.

In the in vivo experiment, six mice were randomly divided into two groups: Lv-shNC group ($N = 3$), Lv-shlincRNA-p21 group ($N = 3$). Corresponding lentiviruses were locally injected into the right maxillary first molar regions of the mice every 3 days (3×10^6 transducing units/mouse). At the 9th day, all animals were sacrificed. Then, the total RNA in the right maxillary alveolar bone was extracted, and qRT-PCR was performed to assess the expression levels of lincRNA-p21.

2.11 | Micro-computed tomography analyses

A high-resolution Inveon Micro-CT (Siemens, Munich, Germany) was used to scan the maxillary specimens. Three-dimensional data were reconstructed using the Inveon Research Workplace 3.0 software (Siemens).

2.12 | Histology and eosin staining and tartrate-resistant acid phosphatase staining

After decalcification in 10% ethylenediaminetetraacetic acid (pH 7.4) for 2 weeks, the maxillae samples were dehydrated and embedded in paraffin. Consecutive 5-µm transverse sections of the maxillary first molar region were obtained. The first investigator (Y. Yang), who encoded and allocated all sections, was the only one aware of the group allocation and did not participate in the following experiments. Then, after the sections were deparaffinized, histology and eosin (H&E) staining was performed following standard processes, and tartrate-resistant acid phosphatase (TRAP) staining was conducted using an acid phosphatase kit (387A-1KT; Sigma, USA) according to the manufacturer's protocols.

2.13 | Immunohistochemical staining

After dewaxing and rehydration, slides were submerged in citric unmasking solution at 95–98°C for 15 min for antigen unmasking. After natural cooling, slides were immersed in 3% hydrogen peroxide for 10 min to quench endogenous peroxidase activity. After that, the sections were blocked

with 5% BSA for 1 h, followed by incubation with a primary antibody at 4°C overnight. After that, the slides were washed with PBS, incubated with a secondary antibody (Zhongshan Goldenbridge Biotechnology Co.) in a humidified chamber at room temperature for 30 min. Then, diaminobenzidine solution was applied to each section, and the sections were monitored closely. Then, the sections were counterstained with hematoxylin and dehydrated.

2.14 | Statistical analysis

All data are presented as the mean ± standard deviation (SD) from triplicate experiments and were analyzed with GraphPad Prism 8.0 (GraphPad Software). Differences between the two groups were analyzed using Student's *t*-test. In the case of three or more groups, single-factor analysis of variance was employed. *p* values <.05 were set as the threshold of statistical significance.

3 | RESULTS

3.1 | Orthodontic force inhibits mineralization of cementoblasts in vivo

To investigate whether mechanical compressive force could suppress the mineralization of cementoblasts, we established an experimental animal model of tooth movement ($N = 5$). The maxillary right first molar was subjected to an orthodontic force (Figure 1A), and the contralateral molar was set as the control tooth. Obvious resorption lacunae and TRAP+osteoclasts were observed on the compressed side of the periodontal tissue after force loading (Figure 1B). In addition, the expression of the mineralization-related protein Ocn decreased in the cementoblasts on the compressed side (Figure 1B).

3.2 | LincRNA-p21 expression is significantly upregulated in cementoblasts subjected to compressive force

To investigate lncRNA expression in immortalized mouse cementoblast-like cells under compressive force, we performed RNA sequencing, and the data showed that a total of 70 lncRNAs were differentially regulated in the force group compared with the control group. Among these lncRNAs, lincRNA-p21 showed strongly upregulated expression (Figure 1D,E). To further study the relationship of lincRNA-p21 expression and mechanical compression, we subjected cementoblasts to 1.5 g/cm^2 of compression force for 0, 2, 4, 6, 8, or 12 h.

The results showed that the expression level of lincRNA-p21 increased at all time points and reached a peak at 4 h (Figure 1F). After that, all durations for force loading were set as 4 h.

3.3 | Knockdown of LincRNA-p21 reverses force-induced mineralization suppression

To further link force-induced lincRNA-p21 expression to force-induced mineralization suppression, we designed three different siRNA sequences for lincRNA-p21, and the third siRNA sequence (silincRNA-p21-3) was the most efficient, with 72.95% silencing (Figure 2A), and was used in subsequent experiments. We knocked down lincRNA-p21 in cementoblasts, and the results from the western blot and qPCR assays revealed that suppressing lincRNA-p21 led to increased expression of mineralization markers (Figure 2C,E, and Figure S1A). In addition, a pQLL vector was used to construct a lincRNA-p21 overexpression plasmid, and overexpressing lincRNA-p21 (144.01 times more than the control group) downregulated mineralization marker expression (Figure 2B,D,E, and Figure S1B), suggesting that lincRNA-p21 is a key player in the mineralization of cementoblasts.

After these experiments, the cells were pretransfected with si-lincRNA-p21 and then exposed to mechanical pressure for 4 h, and the force-induced upregulated expression of lincRNA-p21 was reversed (Figure 2F). The qPCR results and western blot results showed that the downregulation of mineralization marker expression under compressive force was rescued by lincRNA-p21 knockdown (Figure 2F,G, and Figure S1C), indicating that lincRNA-p21 participates in force-induced mineralization suppression.

3.4 | LincRNA-p21 modulates mineralization through autophagy under compressive force

To dissect the mechanism by which mechanical pressure induces lincRNA-p21 to suppress mineralization in cementoblasts, we investigated the autophagic process.

We first measured autophagic flux using a previously reported approach.[18] In this light chain 3 (LC3) turnover assay, autophagosome LC3-Ⅱ was significantly decreased in the force-loaded cementoblasts (Figure 3A and Figure S1D). To distinguish between the inhibited synthetic and enhanced degradative phases of autophagy, we blocked autophagic degradation by the addition of chloroquine (CQ), which neutralizes lysosomal and
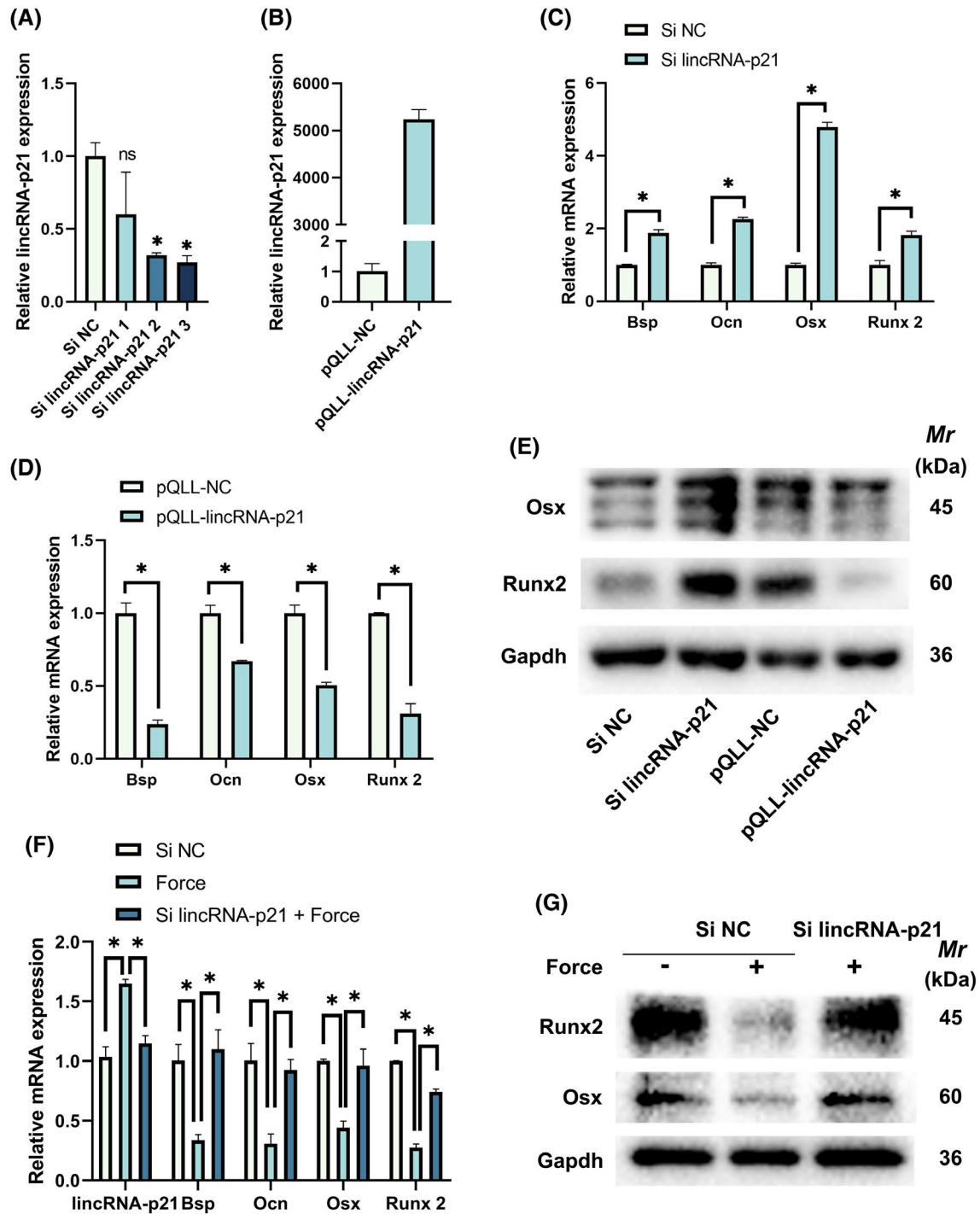
FIGURE 2 Knockdown of lincRNA-p21 rescued the mineralization capability of compressed cementoblasts. Cells were transfected with lincRNA-p21 siRNA (si-lincRNA-p21) or lincRNA-p21 vector (pQLL-lincRNA-p21) to knock down or overexpress its expression. (A) Relative lincRNA-p21 expression in cementoblasts after different siRNAs were transfected; *$p < .05$. (B) Relative lincRNA-p21 expression in cementoblasts after pQLL-NC and pQLL-lincRNA-p21 were transfected; *$p < .05$. (C) Relative mineralization-related mRNA expression in the lincRNA-p21 knockdown groups (*$p < .05$). (D) Relative mineralization-related mRNA expression in the lincRNA-p21 overexpression groups (*$p < .05$). (E) Western blot analyses of the expression of Osx and Runx2 in the lincRNA-p21 knockdown and overexpression groups. (F) Relative lincRNA-p21 and mineralization-related mRNA expression in compressed cementoblasts with lincRNA-p21 knockdown; *$p < .05$. (G) Relative mineralization-related protein expression in compressed cementoblasts with lincRNA-p21 knockdown; *$p < .05$

vacuolar pH, and compared LC3-Ⅱ levels between the force-loaded cementoblasts and the control cementoblasts. Under this condition, the significant decrease in LC3-Ⅱ levels indicated that mechanical compressive force impairs autophagosome synthesis (Figure 3A and Figure S1D).

To determine whether lincRNA-p21 participates in autophagic regulation, we measured the levels of autophagy markers after knocking down or overexpressing lincRNA-p21. The expression of Beclin 1 and LC3-II/I increased when lincRNA-p21 was knocked down, and these biomarkers decreased when lincRNA-p21 was overexpressed (Figure 3B and Figure S1E,F). Another autophagy marker, P62/SQSTM (P62), showed an opposite trend after the expression of lincRNA-p21 was manipulated (Figure 3B and Figure S1E,F). Moreover, immunofluorescence staining demonstrated that LC3 aggregated in cementoblasts when the expression of lincRNA-p21 was inhibited (Figure 3C). LC3 puncta were significantly decreased after transfection with the pQLL-lincRNA-p21 vector (Figure 3C). Furthermore, to test the function of lincRNA-p21 in autophagy, we used the LC3 turnover assay described above in cementoblasts after lincRNA-p21 was knocked down or overexpressed. We found that overexpressing lincRNA-p21 led to a similar pattern as force loading, and knocking down lincRNA-p21 enhanced autophagosome synthesis (Figure 3D and Figure S1G,H).

To further investigate whether lincRNA-p21 mediates the autophagy of cementoblasts under mechanical pressure, we utilized pretransfection with si-lincRNA-p21 to reverse the force-induced upregulation of lincRNA-p21 expression. LncRNA interference reversed the force-induced downregulation of Beclin 1 and LC3-II/I expression (Figure 3E and Figure S2A). In addition, knockdown of lincRNA-p21 alleviated the hindrance of mechanical pressure on the degradation of p62 (Figure 3E and Figure S2A). These results indicated that force-induced lincRNA-p21 impaired the autophagic process in cementoblasts.

To determine whether lincRNA-p21 modulates mineralization through autophagy, we treated cementoblasts pretransfected with si-lincRNA-p21 with the autophagy inhibitor 3-methyladenine (3-MA), and the cementoblasts pretransfected with pQLL-lincRNA-p21 were treated with the autophagy activator rapamycin (Rapa). The increase in mineralization markers induced by lincRNA-p21 knockdown was abolished by the autophagy inhibitor 3-MA, and the lincRNA-p21-mediated suppression of mineralization was partially relieved by the autophagy activator Rapa (Figure 3F,G and Figure S2B,C).

Together, the results shown in Figure 3 suggest that force-induced lincRNA-p21 inhibits mineralization by impairing autophagy.

3.5 | LincRNA-p21 inhibits autophagy via interaction with FoxO3

To gain insight into the molecular mechanism of how lincRNA-p21 impairs autophagy, we first examined the

distribution of this lncRNA using subcellular fractionation qPCR. Over 98% of Malat1 was distributed in the nucleus, and approximately 60% of Gapdh was found in the cytoplasm (Figure 4A). These results suggested that cytoplasmic and nuclear distributions were clearly distinguished. We found that over 80% of lincRNA-p21 was located in the nucleus (Figure 4A), indicating that lincRNA-p21 plays a biological role in transcriptional regulation or chromatin interactions.[19,20]

Pathway analysis of RNA sequencing data of the force-loading cementoblasts demonstrated that the FoxO signaling pathway was significantly affected under compressive force (Figure 4B). Given that FoxO transcription factors play a crucial role in autophagic regulation,[21] the interaction probabilities of lincRNA-p21 and transcription factor FoxO3 were calculated (http://pridb.gdcb.iastate.edu/RPISeq/), and potential binding between lincRNA-p21 and FoxO3 was found (random forest [RF]: 0.7, support vector machine [SVM]: 0.9; RF or SVM scores >0.5 were considered "positive").[22] Furthermore, to identify the probable binding region between lincRNA-p21 and FoxO3, we applied the CatRAPID online program (http://service.tartaglialab.com/page/catrapid_group), an algorithm to facilitate the rapid identification of protein-RNA interactions and domains based on secondary structure, hydrogen bonding, and van der Waals contributions.[23] CatRAPID is up to 89% accurate for the prediction of protein-RNA interaction propensities based on the ncRNA-protein interaction database NPinter (http://service.tartaglialab.com/static_files/shared/documentation.html). This analysis demonstrated that the 51–102 protein residue region and the 2501 bp–2626 bp region of lincRNA-p21 were the most likely to interact (Figure 4C,D). Then, a RIP assay was performed in cementoblasts, and significantly higher relative RNA binding was observed between lincRNA-p21 and FoxO3 than IgG (Figure 4E), consistent with prior CatRAPID prediction. These results confirmed the direct binding between lincRNA-p21 and the transcription factor FoxO3.

Furthermore, three different siRNAs for FoxO3 were designed, and the first siRNA sequence (siFoxO3-1) was the most efficient (85.37% was silenced, Figure 4F) and was used in subsequent experiments. Knockdown of FoxO3 abolished lincRNA-p21 knockdown-enhanced autophagy (Figure 4G and Figure S2D), indicating that lincRNA-p21 modulates autophagy by interfering with FoxO3.

3.6 | Knockdown of LincRNA-p21 enhances autophagy and mineralization in vivo

To confirm all of the above in vitro cell experimental data in the in vivo mouse tooth movement model, we established
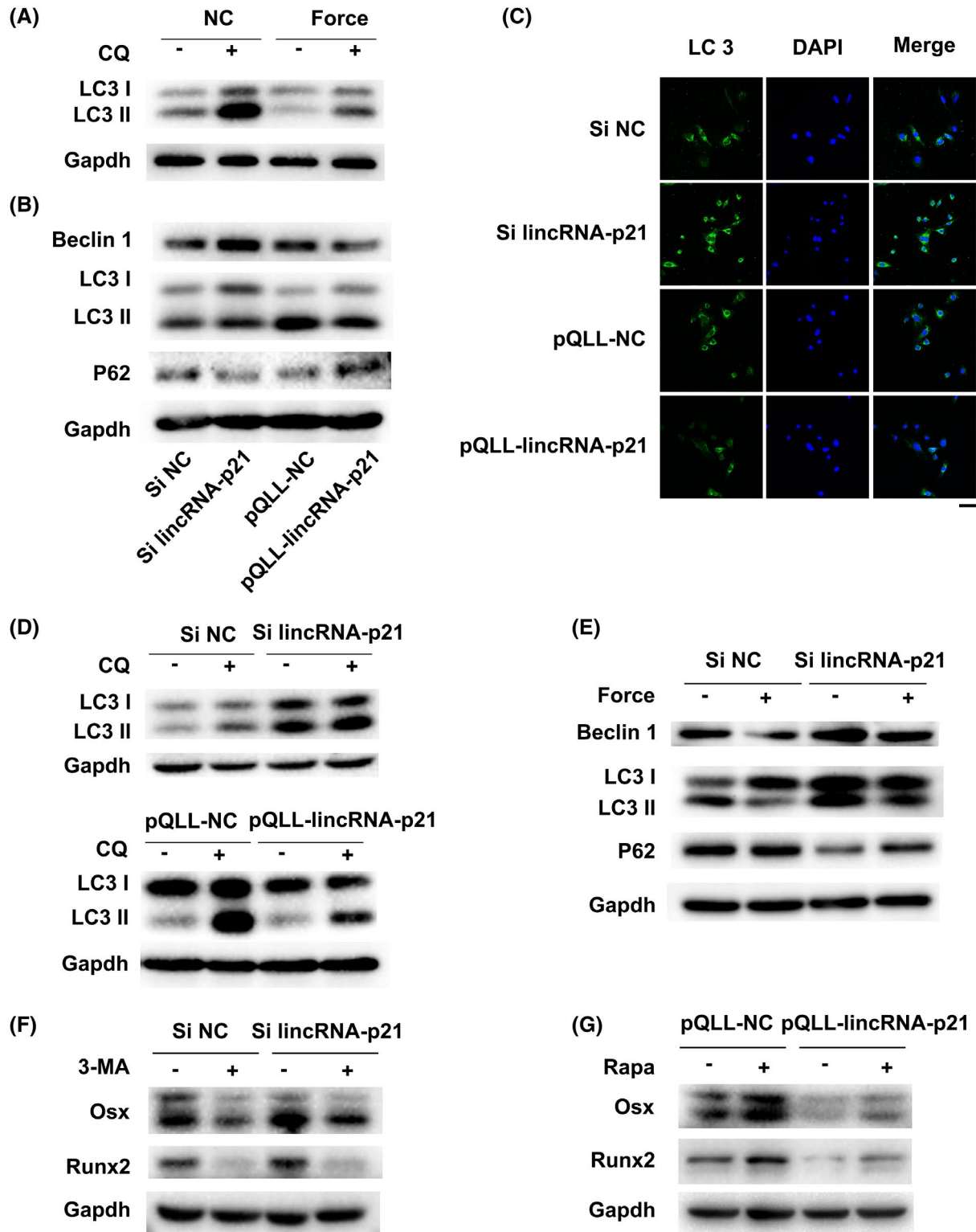
FIGURE 3 Compressive force-induced lincRNA-p21 inhibited mineralization by impeding autophagy. (A) Western blots of LC3 Ⅰ/Ⅱ and GAPDH from compressed cementoblasts and control cells in the absence or presence of chloroquine (CQ, 20 μM for 4 h). (B) Western blots of Beclin1, LC3 Ⅰ/Ⅱ, and p62 in the lincRNA-p21 knockdown and overexpression groups. (C) Pictures of LC3 immunofluorescence staining. Scale bar: 50 μm. (D) Western blots of LC3 Ⅰ/Ⅱ and Gapdh from the lincRNA-p21 knockdown and overexpression cementoblasts in the absence or presence of CQ (20 μM for 4 h). (E) Western blots of Beclin1, LC3 Ⅰ/Ⅱ, and p62 in compressed cementoblasts with the lincRNA-p21 knockdown. (F) Western blots of Osx and Runx2 in lincRNA-p21 knockdown cementoblasts with or without 3-methyladenine (3-MA, 0.15 mM for 24 h) treatment. (G) Western blots of Osx and Runx2 in lincRNA-p21-overexpressing cementoblasts with or without rapamycin (Rapa, 5 μg/ml for 24 h) treatment
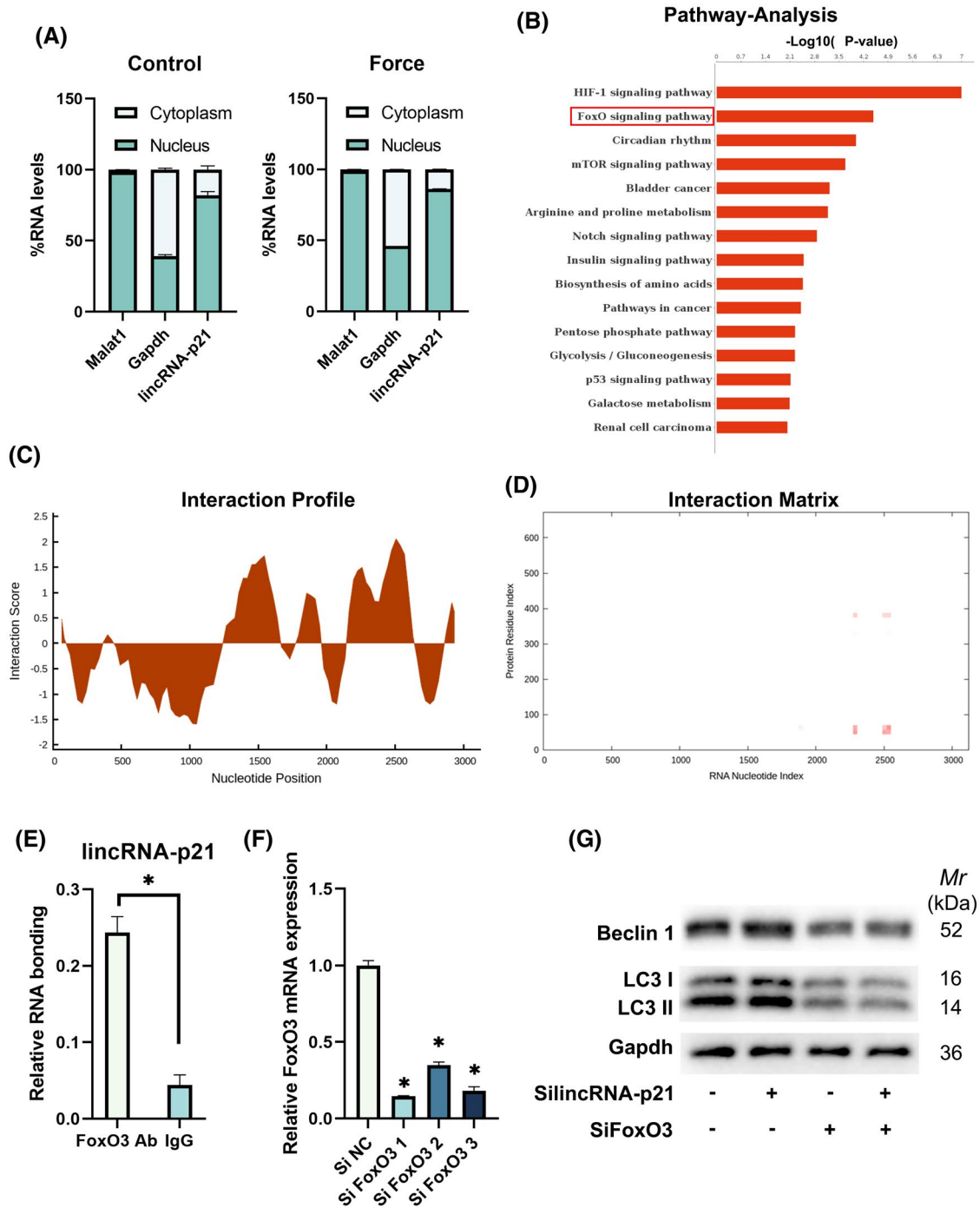
FIGURE 4 LincRNA-p21 functions via the transcription factor FoxO3 in cementoblasts. (A) The expression level of lincRNA-p21 in the subcellular fractions of cementoblasts with or without compressive force loading. (B) The top 15 enrichments in the pathway analysis of differentially expressed genes in cementoblasts subjected to compressive force. (C) The interaction profile, which shows the protein interaction score (Y axis) relative to the lincRNA-p21 RNA sequence (X axis), provides information about the lncRNA regions most likely to be bound by the protein. (D) The FoxO3 protein (Y axis) and lincRNA-p21 RNA (X axis) regions predicted to interact are shown in this heatmap. The red shades indicate the interaction score of the individual amino acid and nucleotide pairs. (E) RIP assays validating lincRNA-p21 binding to FoxO3 (*$p < .05$). (F) Relative FoxO3 mRNA expression after different siRNAs were transfected; *$p < .05$. (G) Western blots of Beclin1 and LC3 I/II in cementoblasts with both lincRNA-p21 and FoxO3 knockdown

a lentiviral infection system (Lv-shlincRNA-p21 and Lv-shNC) to interfere with lincRNA-p21. LincRNA-p21 expression was significantly inhibited in the cementoblasts

infected with Lv-shlincRNA-p21 compared with those infected with Lv-shNC (Figure 5A,B). Consistently, less lincRNA-p21 was detected in mice administrated with

FIGURE 5 Lentiviral infection system knocked down lincRNA-p21 both in vitro and in vivo. (A) Representative images of GFP expression in cementoblasts infected with Lv-shNC and Lv-shlincRNA-p21. Scale bar: 100 μm. (B) Relative lincRNA-p21 expression after Lv-shlincRNA-p21 and Lv-shNC infection in vitro (*$p < .05$). (C) Relative lincRNA-p21 expression after Lv-shlincRNA-p21 and Lv-shNC injection in vivo (*$p < .05$). (D) Schedule diagram of the animal experiment. Orthodontic force was applied to mice in two groups for nine days. Injection of Lv-shNC or Lv-shlincRNA-p21 was performed every three days. (E) The red arrow shows the lentiviral injection site. (F) The tooth movement distances in Force + Lv-NC group and Force + Lv-shlincRNA-p21 group (*$p < .05$)
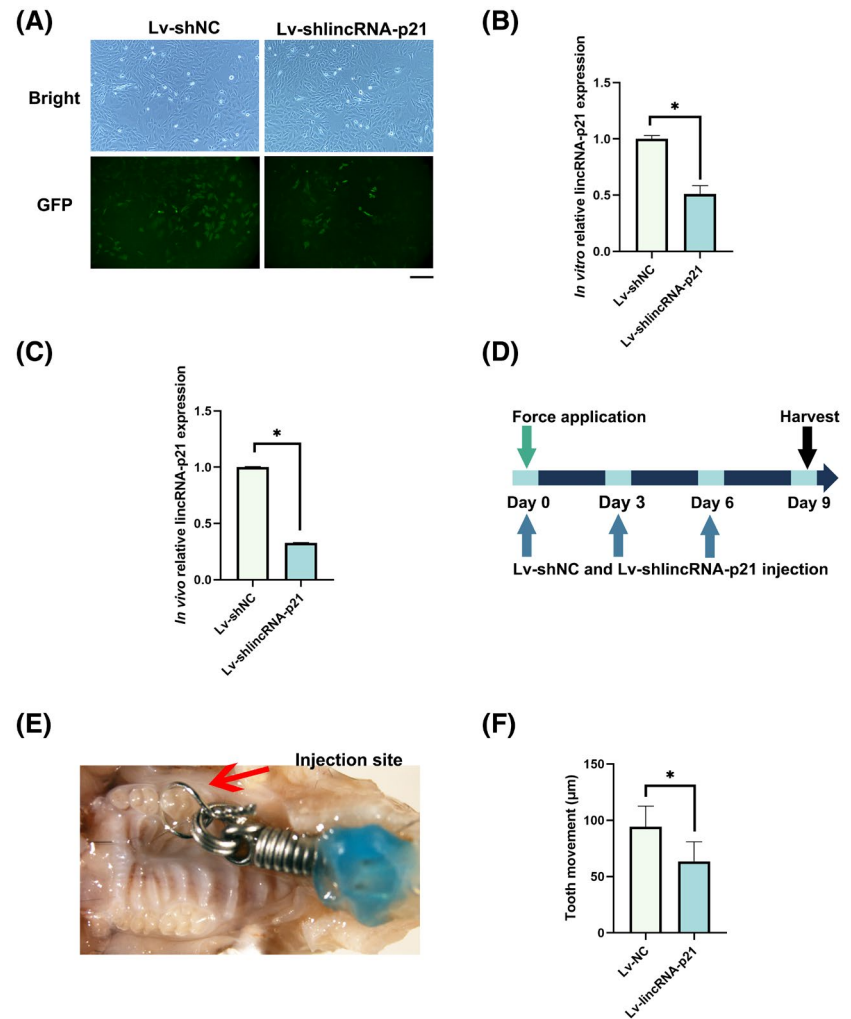
Lv-shlincRNA-p21 ($N = 3$) compared with those treated with Lv-shNC ($N = 3$, Figure 5C), suggesting that this lentiviral infection system functions well in vivo.

To further investigate the function of lincRNA-p21 in vivo, we randomly divided 15 mice into 3 groups: control group ($N = 5$), force + Lv-shNC group ($N = 5$), and force + Lv-shlincRNAp21 group ($N = 5$). The force-loading approach was described above. The force + Lv-shNC group and force + Lv-shlincRNAp21 group were subjected to the corresponding lentiviral vectors by local injection every 3 days (Figure 5D,E). All samples were harvested on the 9th day. These photos demonstrated the successful mesial movement of the first molar (Figure 6A). The tooth movement distances were significantly larger in the force + Lv-shNC group (94.2 ± 18.3 μm) than in the force + Lv-shlincRNA-p21 group (63.6 ± 17.4 μm, Figure 5F). H&E staining showed that orthodontic force led to significant tooth resorption, and local Lv-shlincRNA-p21 injection alleviated this injury, although not to the levels detected in the control group (Figure 6A). In addition, TRAP staining demonstrated the resorption position more clearly, and less resorption was observed

in the force + Lv-shlincRNAp21 group (Figure 6A). Furthermore, the expression of the autophagy protein LC3 and the mineralization marker Ocn decreased in the cementoblasts after force loading, while the reduction in lincRNA-p21 partially rescued autophagic dysfunction and damaged mineralization (Figure 6B).

4 | DISCUSSION

The mineralization of cementoblasts plays an essential role in cementum repair during orthodontic tooth movement.[3] Past studies have shown that mineralization is regulated by mechanical compression in osteoblasts[24] and periodontal ligament cells.[25] However, it remains unclear whether and how mechanical force stimuli regulate mineralization in cementoblasts. The results presented herein suggest a novel mechanism by which mechanical pressure impairs the mineralization capacity of cementoblasts by upregulating lincRNA-p21 expression. First, lincRNA-p21 expression was upregulated in cementoblasts under mechanical pressure. Then, this increased lincRNA-p21
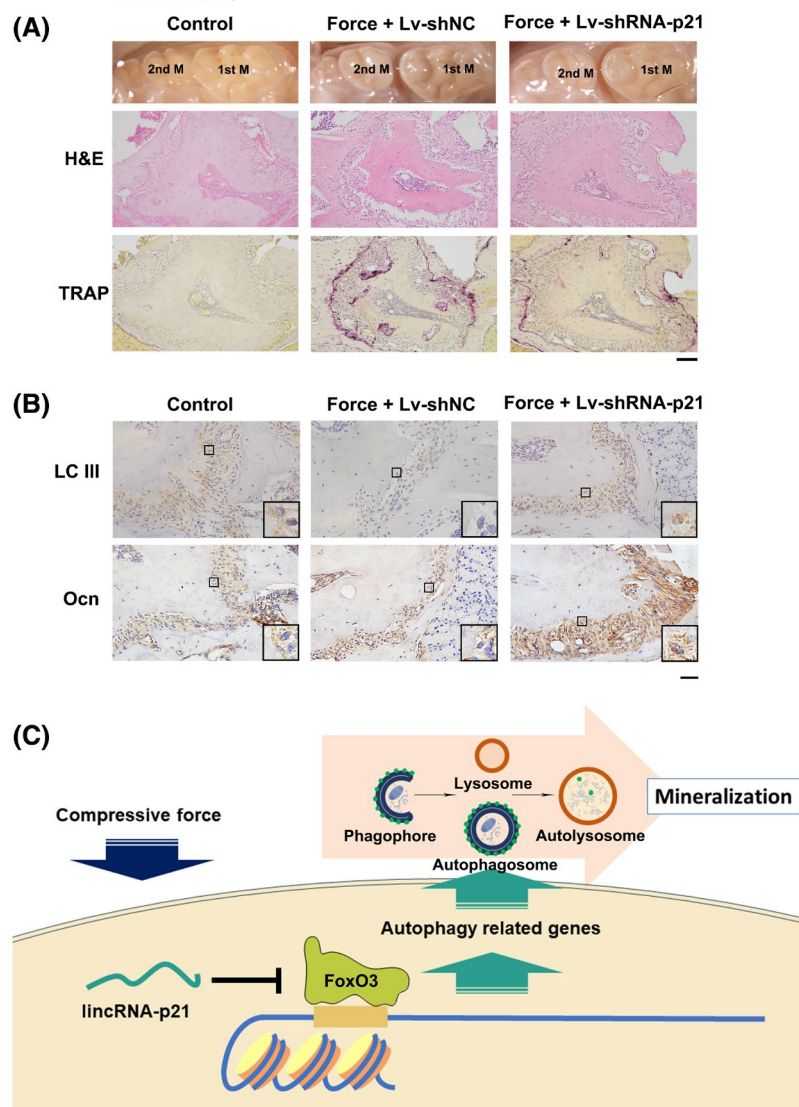
(A)

(B)

(C)

FIGURE 6 Knockdown of lincRNA-p21 alleviated root resorption during orthodontic tooth movement. (A) Pictures showing the successful tooth movement. HE staining and TRAP staining show root resorption. Scale bar: 100 μm. (B) Immunohistochemical staining of LC3 and Ocn. Scale bar: 50 μm (C) Schematic diagram showing that compressive force-induced lincRNA-p21 impedes autophagy-related gene transcription by binding FoxO3 and subsequently impairs mineralization in cementoblasts

expression blocked the expression of autophagy-associated genes by interfering with the transcription factor FoxO3. Finally, the impaired autophagic process reduced the mineralization capacity of cementoblasts.

Recently, extensive sequencing data have demonstrated that many lncRNAs are dysregulated in diverse biological and pathological processes.[26] However, few lncRNAs have been investigated to date. We analyzed the RNA sequencing data of cementoblasts under compressive force and found that lincRNA-p21 was one of the top lncRNAs with upregulated expression.[5] Furthermore, we found that lincRNA-p21 plays an inhibitory role in cementogenesis. In addition, a growing number of studies have shown the regulatory role and functional diversity of lncRNAs in mineralization; thus, lncRNAs are regarded as potential therapeutic targets of disease progression.[27,28] For example, lncRNA TUG1 participates in the decreased osteogenesis of bone marrow mesenchymal stem cells after irradiation, and the knockdown of lncRNA TUG1 alleviates this pathological process.[28] The present study indicates that the inhibitory role of lincRNA-p21 in cementogenesis under compressive force provides a promising target to reduce orthodontic-induced tooth resorption.

Autophagy is an important endogenous protective mechanism that maintains cell and tissue homeostasis under environmental stress.[29] Mechanical stress enhances the autophagic process in nucleus pulposus cells,[30] and periodontal ligament cells[10] while inhibiting the autophagic process in skeletal muscle cells.[8] Our study found that mechanical stress impairs autophagy in cementoblasts. This discrepancy in results can be attributed to differences in cell types, force-loading approaches, or force magnitudes. In addition, many studies have indicated that autophagic vacuoles could be utilized as vehicles in osteoblasts to secrete apatite crystals, and defective autophagy results in bone loss.[11] Accumulating evidence has shown that autophagy is a potential therapeutic target for osteogenesis-related diseases.[12] Considering that cementoblasts share many characteristics with osteoblasts, we hypothesized that autophagy is involved in cementogenic dysfunction in

cementoblasts under compressive force. The present study shows that autophagy plays an essential role in mineralization, consistent with the previous studies.

Past investigations have shown diverse cellular functions and various mechanisms of lincRNA-p21. LincRNA-p21 can stabilize HIF-1α by disrupting the VHL-HIF-1α interaction and promoting glycolysis.[16] The interaction of lincRNA-p21 with STAT3 transcriptionally impeded STAT3-regulated downstream gene expression in head and neck squamous cell carcinoma.[31] However, whether and how lincRNA-p21 is involved in cementogenic capacity via autophagy under compressive force remains obscure. Our findings demonstrated that compression-induced lincRNA-p21 impedes the autophagic process in cementoblasts, which is not consistent with the results of a recent finding that bilobalide-induced lincRNA-p21 promotes autophagy in microglial cells.[32] These results indicate the controversy over the role of lincRNA-p21 in autophagy in various cell types and demonstrate that lncRNAs are complex and have diverse functions.

To uncover the mechanism by which lincRNA-p21 regulates autophagy, we performed pathway analysis of force-loaded cementoblast RNA sequencing data. The results indicate the possible regulatory role of the forkhead box O (FoxO) signaling pathway in force-loading cementoblasts. The present investigation confirmed the interaction between lincRNA-p21 and FoxO3, one member of the FoxO family. This transcription factor subfamily, including FoxO1, FoxO3, FoxO4, and FoxO6, regulates cell differentiation, metabolism, proliferation, and survival in mammals.[33] Previous studies have reported that FoxO3 enhances autophagy in other cells, including skeletal muscle cells,[34] mesenchymal stem cells,[35] hematopoietic stem cells,[36] and developing hippocampal neurons.[37] For example, Mammucari et al. found that FoxO3 controls the transcription of autophagy-related genes, and regulates the effect of FoxO3 on autophagy in skeletal muscle cells.[34] These findings are consistent with our results that the knockdown of FoxO3 negated the autophagy promoted by lincRNA-p21 deficiency. In contrast, Lin et al. showed that downregulation of FoxO3 expression induces the transcriptional activity of autophagy-related genes and triggers the autophagic signaling pathway in liver tumor tissue,[38] indicating the complex role of FoxO3 in autophagy in different tissues and physiological conditions.

Besides, lincRNA-p21 was reported to play a regulatory role in the HIF-1 signaling pathway under hypoxia conditions.[16,39] The significant upregulation of the HIF-1 signaling pathway was also demonstrated in our pathway analysis (Figure 4B). The activation of the HIF-1 signaling pathway is essential to maintain cell homeostasis and metabolism in the event of oxygen deficiency. HIF-1 signal pathway increases oxygen availability by promoting

angiogenesis and erythropoiesis.[40] And hypoxia was induced by the force-loading method used in the present study. Consistently, in vivo, local hypoxia is also induced at the compressed side during orthodontic tooth movement.[41] Hypoxia and mechanical pressure play a synergistic role throughout the orthodontic tooth movement. It is difficult to completely distinguish the effects of these two environmental stimuli. To better simulate the environment at the compressed side during orthodontic tooth movement, light force (1.5 g/cm^2), and shorter loading time (4 h) were used.

To confirm the role of lincRNA-p21 during orthodontic tooth movement in an experimental model, lentiviral vectors were administrated locally to inhibit the expression of lincRNA-p21 during tooth movement. These results showed knockdown of lincRNA-p21 relieved impeded autophagic process, enhanced impaired cementogenesis, and alleviated force-induced root resorption partially. However, a potential limitation is that local lentiviral administration inhibited lincRNA-p21 expression in periodontal ligament cells and osteoblasts of alveolar bone as well, instead of cementoblasts only. This is a probable reason why the knockdown of lincRNA-p21 inhibited orthodontic tooth movement. Rapa, an autophagy inducer, was also reported to increase bone density and slow down orthodontic tooth movement.[10,42] This indicates the possible regulatory role of lincRNA-p21 in the autophagy process of periodontal ligament cells and osteoblasts. The underlying mechanisms remain for further investigations.

In conclusion, for the first time, we showed that lincRNA-p21, induced by mechanical compression, decreases the autophagic process and subsequently impairs the cementogenic process (Figure 6C). In addition, we found that lincRNA-p21 sequesters FoxO3 from its target autophagy-related genes by direct binding. Our study suggests a novel mechanism of cementogenesis by lncRNAs during orthodontic tooth movement.

DISCLOSURES
The authors declare no conflict of interests.

AUTHOR CONTRIBUTIONS
Hao Liu contributed to the conception, design, data acquisition, analysis, interpretation, and drafted the manuscript. Yiping Huang contributed to the conception, design, data acquisition, analysis, interpretation, and critically revised the manuscript. Yuhui Yang, Yineng Han contributed to data acquisition, analysis, interpretation,

and critically revised the manuscript. Lingfei Jia, Weiran Li contributed to conception, design, analysis, interpretation, and critically revised the manuscript. All authors gave final approval and agree to be accountable for all aspects of the work.

ORCID

Hao Liu https://orcid.org/0000-0003-2467-6729
Weiran Li https://orcid.org/0000-0001-9895-1143

REFERENCES

1. Killiany DM. Root resorption caused by orthodontic treatment: an evidence-based review of literature. *Semin Orthod*. 1999;5(2):128-133. doi:10.1016/s1073-8746(99)80032-2

2. Castro IO, Alencar AH, Valladares-Neto J, Estrela C. Apical root resorption due to orthodontic treatment detected by cone beam computed tomography. *Angle Orthod*. 2013;83(2):196-203. doi:10.2319/032112-240.1

3. Iglesias-Linares A, Hartsfield JK Jr. Cellular and molecular pathways leading to external root resorption. *J Dent Res*. 2017;96(2):145-152. doi:10.1177/0022034516677539

4. Feller L, Khammissa RA, Thomadakis G, Fourie J, Lemmer J. Apical external root resorption and repair in orthodontic tooth movement: biological events. *Biomed Res Int*. 2016;2016:4864195. doi:10.1155/2016/4864195

5. Liu H, Huang Y, Zhang Y, et al. Long noncoding RNA expression profile of mouse cementoblasts under compressive force. *Angle Orthod*. 2019;89(3):455-463. doi:10.2319/061118-438.1

6. Huang L, Meng Y, Ren A, Han X, Bai D, Bao L. Response of cementoblast-like cells to mechanical tensile or compressive stress at physiological levels in vitro. *Mol Biol Rep*. 2009;36(7):1741-1748. doi:10.1007/s11033-008-9376-3

7. Kroemer G, Mariño G, Levine B. Autophagy and the integrated stress response. *Mol Cell*. 2010;40(2):280-293. doi:10.1016/j.molcel.2010.09.023

8. Teng BT, Pei XM, Tam EW, Benzie IF, Siu PM. Opposing responses of apoptosis and autophagy to moderate compression in skeletal muscle. *Acta Physiol (Oxford, England)*. 2011;201(2):239-254. doi:10.1111/j.1748-1716.2010.02173.x

9. Mariño G, Niso-Santano M, Baehrecke EH, Kroemer G. Self-consumption: the interplay of autophagy and apoptosis. *Nat Rev Mol Cell Biol*. 2014;15(2):81-94. doi:10.1038/nrm3735

10. Chen L, Mo S, Hua Y. Compressive force-induced autophagy in periodontal ligament cells downregulates osteoclastogenesis during tooth movement. *J Periodontol*. 2019;90(10):1170-1181. doi:10.1002/jper.19-0049

11. Nollet M, Santucci-Darmanin S, Breuil V, et al. Autophagy in osteoblasts is involved in mineralization and bone homeostasis. *Autophagy*. 2014;10(11):1965-1977. doi:10.4161/auto.36182

12. Zhang Y, Li M, Liu Z, Fu Q. Arbutin ameliorates glucocorticoid-induced osteoporosis through activating autophagy in osteoblasts. *Exp Biol Med (Maywood, NJ)*. 2021;246(14):1650-1659. doi:10.1177/15353702211002136

13. Peng WX, Koirala P, Mo YY. LncRNA-mediated regulation of cell signaling in cancer. *Oncogene*. 2017;36(41):5661-5667. doi:10.1038/onc.2017.184

14. Lu Q, Xu W, Liu L, et al. Traumatic compressive stress inhibits osteoblast differentiation through long chain non-coding RNA Dancr. *J Periodontol*. 2020;91(11):1532-1540. doi:10.1002/jper.19-0648

15. Huarte M, Guttman M, Feldser D, et al. A large intergenic noncoding RNA induced by p53 mediates global gene repression in the p53 response. *Cell*. 2010;142(3):409-419. doi:10.1016/j.cell.2010.06.040

16. Yang F, Zhang H, Mei Y, Wu M. Reciprocal regulation of HIF-1α and lincRNA-p21 modulates the Warburg effect. *Mol Cell*. 2014;53(1):88-100. doi:10.1016/j.molcel.2013.11.004

17. Jin A, Hong Y, Yang Y, et al. FOXO3 mediates tooth movement by regulating force-induced osteogenesis. *J Dent Res*. 2021;220345211021534:220345211021534. doi:10.1177/00220345211021534

18. Mizushima N, Yoshimori T, Levine B. Methods in mammalian autophagy research. *Cell*. 2010;140(3):313-326. doi:10.1016/j.cell.2010.01.028

19. Batista PJ, Chang HY. Long noncoding RNAs: cellular address codes in development and disease. *Cell*. 2013;152(6):1298-1307. doi:10.1016/j.cell.2013.02.012

20. Xiao M, Cui SU, Zhang L, et al. AC138128.1 an intronic lncRNA originating from ERCC1 implies a potential application in lung cancer treatment. *J Cancer*. 2019;10(16):3608-3617. doi:10.7150/jca.31832

21. Cheng Z. The FoxO-autophagy axis in health and disease. *Trends Endocrinol Metab*. 2019;30(9):658-671. doi:10.1016/j.tem.2019.07.009

22. Muppirala UK, Honavar VG, Dobbs D. Predicting RNA-protein interactions using only sequence information. *BMC Bioinformatics*. 2011;12:489. doi:10.1186/1471-2105-12-489

23. Royce-Tolland ME, Andersen AA, Koyfman HR, et al. The A-repeat links ASF/SF2-dependent Xist RNA processing with random choice during X inactivation. *Nat Struct Mol Biol*. 2010;17(8):948-954. doi:10.1038/nsmb.1877

24. Wang D, Wang H, Gao F, Wang K, Dong F. ClC-3 promotes osteogenic differentiation in MC3T3-E1 cell after dynamic compression. *J Cell Biochem*. 2017;118(6):1606-1613. doi:10.1002/jcb.25823

25. Jia RU, Yi Y, Liu J, et al. Cyclic compression emerged dual effects on the osteogenic and osteoclastic status of LPS-induced inflammatory human periodontal ligament cells according to loading force. *BMC Oral Health*. 2020;20(1):7. doi:10.1186/s12903-019-0987-y

26. Harrow J, Frankish A, Gonzalez JM, et al. GENCODE: the reference human genome annotation for The ENCODE Project. *Genome Res*. 2012;22(9):1760-1774. doi:10.1101/gr.135350.111

27. Wang Z, Huang Y, Tan L. Downregulation of lncRNA DANCR promotes osteogenic differentiation of periodontal ligament stem cells. *BMC Dev Biol*. 2020;20(1):2. doi:10.1186/s12861-019-0206-8

28. Zhang W, Chen LI, Wu J, et al. Long noncoding RNA TUG1 inhibits osteogenesis of bone marrow mesenchymal stem cells via Smad5 after irradiation. *Theranostics*. 2019;9(8):2198-2208. doi:10.7150/thno.30798

29. Sil P, Wong SW, Martinez J. More than skin deep: autophagy is vital for skin barrier function. *Front Immunol*. 2018;9:1376. doi:10.3389/fimmu.2018.01376

30. Li Z, Wang J, Deng X, Huang D, Shao Z, Ma K. Compression stress induces nucleus pulposus cell autophagy by inhibition of the PI3K/AKT/mTOR pathway and activation of the JNK pathway. *Connect Tissue Res*. 2021;62(3):337-349. doi:10.1080/03008 207.2020.1736578

31. Jin S, Yang X, Li J, Yang W, Ma H, Zhang Z. p53-targeted lincRNA-p21 acts as a tumor suppressor by inhibiting JAK2/STAT3 signaling pathways in head and neck squamous cell carcinoma. *Mol Cancer*. 2019;18(1):38. doi:10.1186/s1294 3-019-0993-3

32. Zhao B, Peng Q, Poon EHL, et al. Leonurine promotes the osteoblast differentiation of rat BMSCs by activation of autophagy via the PI3K/Akt/mTOR pathway. *Front Bioeng Biotechnol*. 2021;9:615191. doi:10.3389/fbioe.2021.615191

33. Accili D, Arden KC. FoxOs at the crossroads of cellular metabolism, differentiation, and transformation. *Cell*. 2004;117(4):421-426. doi:10.1016/s0092-8674(04)00452-0

34. Mammucari C, Milan G, Romanello V, et al. FoxO3 controls autophagy in skeletal muscle in vivo. *Cell Metab*. 2007;6(6):458-471. doi:10.1016/j.cmet.2007.11.001

35. Gómez-Puerto MC, Verhagen LP, Braat AK, Lam EW, Coffer PJ, Lorenowicz MJ. Activation of autophagy by FOXO3 regulates redox homeostasis during osteogenic differentiation. *Autophagy*. 2016;12(10):1804-1816. doi:10.1080/15548 627.2016.1203484

36. Warr MR, Binnewies M, Flach J, et al. FOXO3A directs a protective autophagy program in haematopoietic stem cells. *Nature*. 2013;494(7437):323-327. doi:10.1038/nature11895

37. Schäffner I, Minakaki G, Khan MA, et al. FoxO function is essential for maintenance of autophagic flux and neuronal morphogenesis in adult neurogenesis. *Neuron*. 2018;99(6):1188-1203.e6. doi:10.1016/j.neuron.2018.08.017

38. Lin Z, Niu Y, Wan A, et al. RNA m(6) A methylation regulates sorafenib resistance in liver cancer through FOXO3-mediated autophagy. *EMBO J*. 2020;39(12):e103181. doi:10.15252/embj.2019103181

39. Meng S-S, Xu X-P, Chang W, et al. LincRNA-p21 promotes mesenchymal stem cell migration capacity and survival through hypoxic preconditioning. *Stem Cell Res Ther*. 2018;9(1):280. doi:10.1186/s13287-018-1031-x

40. Lee JW, Bae SH, Jeong JW, Kim SH, Kim KW. Hypoxia-inducible factor (HIF-1)alpha: its protein stability and biological functions. *Exp Mol Med*. 2004;36(1):1-12. doi:10.1038/emm.2004.1

41. Niklas A, Proff P, Gosau M, Römer P. The role of hypoxia in orthodontic tooth movement. *Int J Dent*. 2013;2013: 841840. doi:10.1155/2013/841840

42. Li Y, Jacox LA, Coats S, et al. Roles of autophagy in orthodontic tooth movement. *Am J Orthod Dentofac Orthop*. 2021;159(5):582-593. doi:10.1016/j.ajodo.2020.01.027

SUPPORTING INFORMATION

Additional supporting information may be found in the online version of the article at the publisher's website.